



Observation of double $c\bar{c}$ production in e^+e^- annihilation at $\sqrt{s} \approx 10.6$ GeV

K. Abe,¹⁰ K. Abe,⁴³ R. Abe,³⁰ T. Abe,⁴⁴ I. Adachi,¹⁰ Byoung Sup Ahn,¹⁷ H. Aihara,⁴⁵ M. Akatsu,²³ Y. Asano,⁵⁰ T. Aso,⁴⁹ V. Aulchenko,² T. Aushev,¹⁴ A. M. Bakich,⁴⁰ Y. Ban,³⁴ E. Banas,²⁸ W. Bartel,⁶ A. Bay,²⁰ P. K. Behera,⁵¹ A. Bondar,² A. Bozek,²⁸ M. Bračko,^{21,15} J. Brodzicka,²⁸ T. E. Browder,⁹ B. C. K. Casey,⁹ P. Chang,²⁷ Y. Chao,²⁷ B. G. Cheon,³⁹ R. Chistov,¹⁴ S.-K. Choi,⁸ Y. Choi,³⁹ M. Danilov,¹⁴ L. Y. Dong,¹² J. Dragic,²² A. Drutskoy,¹⁴ S. Eidelman,² V. Eigens,¹⁴ Y. Enari,²³ C. Fukunaga,⁴⁷ N. Gabyshev,¹⁰ A. Garmash,^{2,10} T. Gershon,¹⁰ A. Gordon,²² R. Guo,²⁵ F. Handa,⁴⁴ T. Hara,³² Y. Harada,³⁰ N. C. Hastings,²² H. Hayashii,²⁴ M. Hazumi,¹⁰ E. M. Heenan,²² I. Higuchi,⁴⁴ T. Higuchi,⁴⁵ T. Hojo,³² T. Hokuue,²³ Y. Hoshi,⁴³ K. Hoshina,⁴⁸ S. R. Hou,²⁷ W.-S. Hou,²⁷ H.-C. Huang,²⁷ T. Igaki,²³ Y. Igarashi,¹⁰ T. Iijima,²³ K. Inami,²³ A. Ishikawa,²³ R. Itoh,¹⁰ M. Iwamoto,³ H. Iwasaki,¹⁰ Y. Iwasaki,¹⁰ H. K. Jang,³⁸ J. Kaneko,⁴⁶ J. H. Kang,⁵⁴ J. S. Kang,¹⁷ P. Kapusta,²⁸ N. Katayama,¹⁰ H. Kawai,³ Y. Kawakami,²³ N. Kawamura,¹ T. Kawasaki,³⁰ H. Kichimi,¹⁰ D. W. Kim,³⁹ Heejong Kim,⁵⁴ H. J. Kim,⁵⁴ H. O. Kim,³⁹ Hyunwoo Kim,¹⁷ S. K. Kim,³⁸ T. H. Kim,⁵⁴ K. Kinoshita,⁵ P. Krokovny,² R. Kulasiri,⁵ S. Kumar,³³ A. Kuzmin,² Y.-J. Kwon,⁵⁴ J. S. Lange,^{7,36} G. Leder,¹³ S. H. Lee,³⁸ J. Li,³⁷ D. Liventsev,¹⁴ R.-S. Lu,²⁷ J. MacNaughton,¹³ G. Majumder,⁴¹ F. Mandl,¹³ S. Matsumoto,⁴ T. Matsumoto,^{23,47} H. Miyake,³² H. Miyata,³⁰ G. R. Moloney,²² T. Mori,⁴ T. Nagamine,⁴⁴ Y. Nagasaka,¹¹ E. Nakano,³¹ M. Nakao,¹⁰ J. W. Nam,³⁹ Z. Natkaniec,²⁸ K. Neichi,⁴³ S. Nishida,¹⁸ O. Nitoh,⁴⁸ S. Noguchi,²⁴ T. Nozaki,¹⁰ S. Ogawa,⁴² F. Ohno,⁴⁶ T. Ohshima,²³ T. Okabe,²³ S. Okuno,¹⁶ S. L. Olsen,⁹ Y. Onuki,³⁰ W. Ostrowicz,²⁸ H. Ozaki,¹⁰ P. Pakhlov,¹⁴ H. Palka,²⁸ C. W. Park,¹⁷ H. Park,¹⁹ K. S. Park,³⁹ L. S. Peak,⁴⁰ J.-P. Perroud,²⁰ M. Peters,⁹ L. E. Pilonen,⁵² N. Root,² H. Sagawa,¹⁰ S. Saitoh,¹⁰ Y. Sakai,¹⁰ M. Satapathy,⁵¹ A. Satpathy,^{10,5} O. Schneider,²⁰ S. Schrenk,⁵ C. Schwanda,^{10,13} S. Semenov,¹⁴ K. Senyo,²³ R. Seuster,⁹ M. E. Sevier,²² H. Shibuya,⁴² V. Sidorov,² J. B. Singh,³³ S. Stanič,^{50,*} M. Starič,¹⁵ A. Sugi,²³ A. Sugiyama,²³ K. Sumisawa,¹⁰ T. Sumiyoshi,^{10,47} K. Suzuki,¹⁰ S. Suzuki,⁵³ S. K. Swain,⁹ T. Takahashi,³¹ F. Takasaki,¹⁰ K. Tamai,¹⁰ N. Tamura,³⁰ M. Tanaka,¹⁰ G. N. Taylor,²² Y. Teramoto,³¹ S. Tokuda,²³ T. Tomura,⁴⁵ S. N. Tovey,²² W. Trischuk,^{35,†} T. Tsuboyama,¹⁰ T. Tsukamoto,¹⁰ S. Uehara,¹⁰ K. Ueno,²⁷ Y. Unno,³ S. Uno,¹⁰ S. E. Vahsen,³⁵ G. Varner,⁹ K. E. Varvell,⁴⁰ C. C. Wang,²⁷ C. H. Wang,²⁶ J. G. Wang,⁵² M.-Z. Wang,²⁷ Y. Watanabe,⁴⁶ E. Won,¹⁷ B. D. Yabsley,⁵² Y. Yamada,¹⁰ A. Yamaguchi,⁴⁴ Y. Yamashita,²⁹ M. Yamauchi,¹⁰ H. Yanai,³⁰ J. Yashima,¹⁰ Y. Yuan,¹² Y. Yusa,⁴⁴ Z. P. Zhang,³⁷ V. Zhilich,² and D. Žontar⁵⁰

(Belle Collaboration)

¹Aomori University, Aomori

²Budker Institute of Nuclear Physics, Novosibirsk

³Chiba University, Chiba

⁴Chuo University, Tokyo

⁵University of Cincinnati, Cincinnati OH

⁶Deutsches Elektronen-Synchrotron, Hamburg

⁷University of Frankfurt, Frankfurt

⁸Gyeongsang National University, Chinju

⁹University of Hawaii, Honolulu HI

¹⁰High Energy Accelerator Research Organization (KEK), Tsukuba

¹¹Hiroshima Institute of Technology, Hiroshima

¹²Institute of High Energy Physics, Chinese Academy of Sciences, Beijing

¹³Institute of High Energy Physics, Vienna

¹⁴Institute for Theoretical and Experimental Physics, Moscow

¹⁵J. Stefan Institute, Ljubljana

¹⁶Kanagawa University, Yokohama

¹⁷Korea University, Seoul

¹⁸Kyoto University, Kyoto

¹⁹Kyungpook National University, Taegu

²⁰*Institut de Physique des Hautes Énergies, Université de Lausanne, Lausanne*

²¹*University of Maribor, Maribor*

²²*University of Melbourne, Victoria*

²³*Nagoya University, Nagoya*

²⁴*Nara Women's University, Nara*

²⁵*National Kaohsiung Normal University, Kaohsiung*

²⁶*National Lien-Ho Institute of Technology, Miao Li*

²⁷*National Taiwan University, Taipei*

²⁸*H. Niewodniczanski Institute of Nuclear Physics, Krakow*

²⁹*Nihon Dental College, Niigata*

³⁰*Niigata University, Niigata*

³¹*Osaka City University, Osaka*

³²*Osaka University, Osaka*

³³*Panjab University, Chandigarh*

³⁴*Peking University, Beijing*

³⁵*Princeton University, Princeton NJ*

³⁶*RIKEN BNL Research Center, Brookhaven NY*

³⁷*University of Science and Technology of China, Hefei*

³⁸*Seoul National University, Seoul*

³⁹*Sungkyunkwan University, Suwon*

⁴⁰*University of Sydney, Sydney NSW*

⁴¹*Tata Institute of Fundamental Research, Bombay*

⁴²*Toho University, Funabashi*

⁴³*Tohoku Gakuin University, Tagajo*

⁴⁴*Tohoku University, Sendai*

⁴⁵*University of Tokyo, Tokyo*

⁴⁶*Tokyo Institute of Technology, Tokyo*

⁴⁷*Tokyo Metropolitan University, Tokyo*

⁴⁸*Tokyo University of Agriculture and Technology, Tokyo*

⁴⁹*Toyama National College of Maritime Technology, Toyama*

⁵⁰*University of Tsukuba, Tsukuba*

⁵¹*Utkal University, Bhubaneswer*

⁵²*Virginia Polytechnic Institute and State University, Blacksburg VA*

⁵³*Yokkaichi University, Yokkaichi*

⁵⁴*Yonsei University, Seoul*

We report the observation of prompt J/ψ via double $c\bar{c}$ production from the e^+e^- continuum. In this process one $c\bar{c}$ pair fragments into a J/ψ meson while the remaining pair either produces a bound charmonium state or fragments into open charm. Both cases have been observed: the first by studying the mass spectrum of the system recoiling against the J/ψ , and the second by reconstructing the J/ψ together with a charmed meson. We find cross-sections of $\sigma(e^+e^- \rightarrow J/\psi \eta_c(\gamma)) \times \mathcal{B}(\eta_c \rightarrow \geq 4 \text{ charged}) = (0.033^{+0.007}_{-0.006} \pm 0.009) \text{ pb}$ and $\sigma(e^+e^- \rightarrow J/\psi D^{*+}X) = (0.53^{+0.19}_{-0.15} \pm 0.14) \text{ pb}$, and infer $\sigma(e^+e^- \rightarrow J/\psi c\bar{c})/\sigma(e^+e^- \rightarrow J/\psi X) = 0.59^{+0.15}_{-0.13} \pm 0.12$; in each case the uncertainty quoted second is the systematic error. These results are obtained from a 46.2 fb^{-1} data sample collected near the $\Upsilon(4S)$ resonance, with the Belle detector at the KEKB asymmetric energy e^+e^- collider.

PACS numbers: 13.65.+i, 13.25.Gv, 14.40.Gx

Prompt charmonium production in e^+e^- annihilation provides an opportunity to study both perturbative and non-perturbative effects in QCD. In a previous paper [1] we presented cross-section measurements for prompt J/ψ and $\psi(2S)$ production, and studies of their kinematic properties, which were compared to predictions of the NRQCD [2, 3, 4, 5] model. The BaBar Collaboration has also published results on prompt J/ψ production [6]. NRQCD predicts that prompt J/ψ production at $\sqrt{s} \approx 10.6$ GeV is dominated by $e^+e^- \rightarrow J/\psi gg$, with additional contributions from $J/\psi g$, $J/\psi c\bar{c}$ and other processes. The color-octet $J/\psi g$ signal predicted in Refs [4, 5] is not observed [1]. The results in Refs [1, 6] do not constrain the contributions from $J/\psi gg$ and $J/\psi c\bar{c}$.

We present the results of a search for $J/\psi c\bar{c}$ production, *i.e.* double $c\bar{c}$ production, where the additional $c\bar{c}$ pair fragments into either charmonium or charmed hadrons. Exclusive associated production with a J/ψ meson was proposed in Ref. [7] as a method for searching for the remaining undiscovered charmonium states. Based on a non-perturbative approach the model of Ref. [8] predicts a cross-section of a few pb for $J/\psi \eta_c$ production at $\sqrt{s} \approx 10.6$ GeV. In contrast, recent theoretical estimates of the $J/\psi c\bar{c}$ cross-section are as small as 0.07 pb [3, 5, 9].

This analysis is based on 41.8 fb^{-1} of data at the $\Upsilon(4S)$ and 4.4 fb^{-1} at an energy 60 MeV below the resonance, collected with the Belle detector at the KEKB asymmetric energy storage rings [10]. Belle is a large solid-angle magnetic spectrometer [11]. Charged particles are reconstructed in a 50-layer central drift chamber (CDC) and their impact parameters are determined using a three-layer silicon vertex detector (SVD). Kaon/pion separation is based on specific ionization (dE/dx) in the CDC, time of flight measurements and the response of aerogel Čerenkov counters (ACC). Electron identification is based on a combination of dE/dx measurements, the ACC response and information about the shape, energy deposit and position of the associated shower in the electromagnetic calorimeter (ECL). Muon identification is provided by 14 layers of 4.7 cm thick iron plates interleaved with resistive plate counters. Photons are reconstructed in the ECL as showers with an energy larger than 20 MeV that are not associated with charged tracks.

We use hadronic events separated from QED, $\tau\tau$, two-photon and beam-gas interaction backgrounds by the selection criteria described in Ref. [1]. Charged pion and kaon candidates are well reconstructed tracks that have been positively identified. K_S candidates are reconstructed by combining $\pi^+\pi^-$ pairs with an invariant mass within $10 \text{ MeV}/c^2$ of the nominal K_S mass. We require the distance between the pion tracks at the K_S vertex to be less than 1 cm, the transverse flight distance from the interaction point to be greater than 0.5 cm and the angle between the K_S momentum direction and decay path to be smaller than 0.1 rad. Photons of energy greater than 50 MeV are combined to form $\pi^0 \rightarrow \gamma\gamma$ candidates if their invariant mass lies within $10 \text{ MeV}/c^2$ of the nominal π^0 mass. Such $\gamma\gamma$ pairs are fitted with a π^0 mass constraint to improve the momentum resolution.

The $J/\psi \rightarrow \ell^+\ell^-$ reconstruction procedure is identical to that presented in Ref. [1]. Two positively identified lepton candidates are required to form a common vertex that is less than $500 \mu\text{m}$ from the interaction point in the plane perpendicular to the beam axis. For $J/\psi \rightarrow e^+e^-$, the invariant mass calculation includes the four-momentum of photons detected within 50 mrad of the e^\pm directions, as a partial correction for final state radiation and bremsstrahlung energy loss. QED processes are suppressed by requiring the total charged multiplicity (N_{ch}) to be greater than four. J/ψ mesons from $B\bar{B}$ events are removed by requiring the momentum of the meson in the e^+e^- center of mass (CM) system, $p_{J/\psi}^*$, to be greater than $2.0 \text{ GeV}/c$. The process $e^+e^- \rightarrow \psi(2S)\gamma$ is partially removed by rejecting events with a photon of CM energy $E^* > 3.5 \text{ GeV}$.

The $J/\psi \rightarrow \ell^+\ell^-$ signal region is defined by the mass window $|M_{\ell^+\ell^-} - M_{J/\psi}| < 30 \text{ MeV}/c^2$ ($\approx 2.5\sigma$). The sideband region is defined by $100 < |M_{\ell^+\ell^-} - M_{J/\psi}| < 400 \text{ MeV}/c^2$ and is used to estimate the contribution from the dilepton combinatorial background under the J/ψ peak. The sideband is scaled, parameterizing the background by a quadratic function.

Distributions of the mass of the system recoiling against the J/ψ candidate—the “recoil mass”—after this selection are shown in Fig. 1a, for both signal and sideband regions. The recoil mass is defined as

$$M_{\text{recoil}} = \sqrt{\left(\sqrt{s} - E_{J/\psi}^*\right)^2 - p_{J/\psi}^{*2}}. \quad (1)$$

A clear threshold near $2m_c$ can be seen. To avoid model dependence, we do not perform an acceptance correction. As examples, the Monte Carlo efficiencies for both $e^+e^- \rightarrow J/\psi q\bar{q}$ ($q = u, d, s$) and $J/\psi c\bar{c}$ events are shown in the inset: the variation with M_{recoil} is smooth. For recoil masses smaller than $2.8 \text{ GeV}/c^2$, no significant J/ψ signal is observed: a fit to the dilepton mass spectrum for events in this region gives 16.4 ± 7.8 events.

The region $2m_c \lesssim M_{\text{recoil}} < 2m_D$ is studied in more detail in order to search for production of J/ψ together with an additional charmonium state. We apply a mass constrained fit to the J/ψ candidates before determining $p_{J/\psi}^*$. Monte Carlo simulation predicts that this improves the M_{recoil} resolution by a factor close to two. The resulting recoil mass spectrum in the data is presented in Fig. 1b: a clear peak is observed around $3 \text{ GeV}/c^2$. Since $e^+e^- \rightarrow \gamma^* \rightarrow J/\psi J/\psi$ is forbidden by charge conjugation symmetry, we interpret this peak as $e^+e^- \rightarrow J/\psi \eta_c$. Additional peaks at recoil masses consistent with the χ_{c0} and $\eta_c(2S)$ mass [12] are also seen.

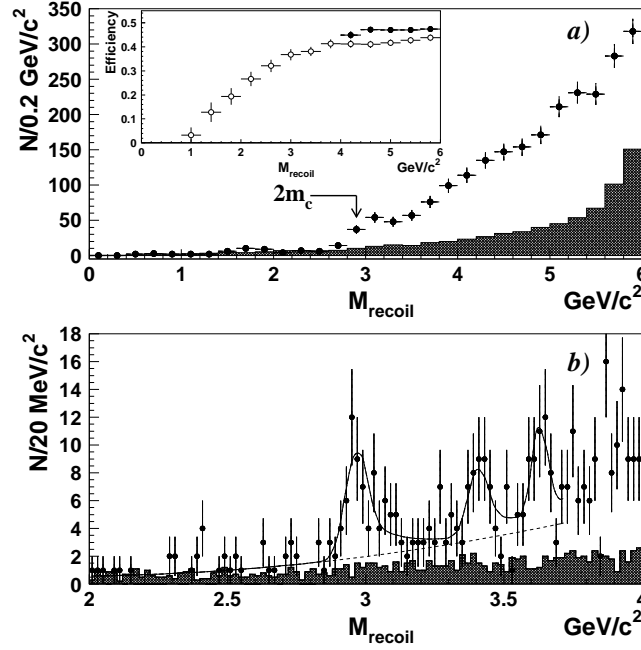


FIG. 1: a) The recoil mass distribution for the J/ψ signal region (points) and scaled sidebands (shaded histogram). The inset shows the MC reconstruction efficiency for $e^+e^- \rightarrow J/\psi q\bar{q}$ ($q = u, d, s$; open circles) and $e^+e^- \rightarrow J/\psi c\bar{c}$ events (closed circles). b) The recoil mass distribution after refitting the J/ψ candidate with a mass constraint for the J/ψ signal region (points) and scaled sidebands (shaded histogram). The curve represents the fit described in the text.

To reproduce the η_c shape in the recoil mass spectrum we generate $e^+e^- \rightarrow \gamma^*(\gamma) \rightarrow J/\psi \eta_c(\gamma)$ Monte Carlo events. We assume p -wave $J/\psi \eta_c$ production, as required by parity conservation, and phase space suppression of $\gamma^* \rightarrow J/\psi \eta_c$ as the virtual γ^* energy varies due to initial state radiation (ISR). This effect produces a high-mass tail in M_{recoil} . The corresponding $\eta_c(2S)$ lineshape is narrower, due to the larger mass of the state and its presumed smaller intrinsic width. The χ_{c0} lineshape assumes s -wave production. The effect of varying the energy dependence of the cross-section in the ISR calculation is included in the systematic error.

A fit to the recoil mass spectrum finds an η_c yield $N_{\eta_c} = 67^{+13}_{-12}$ at a mass $M = (2.962 \pm 0.013) \text{ GeV}/c^2$, with $\chi_{c0}, \eta_c(2S)$ yields $N_{\chi_{c0}} = 39^{+14}_{-13}$, $N_{\eta_c(2S)} = 42^{+15}_{-13}$ at masses $M_{\chi_{c0}} = (3.403 \pm 0.014) \text{ GeV}/c^2$ and $M_{\eta_c(2S)} = (3.622 \pm 0.012) \text{ GeV}/c^2$ respectively. We use a second order polynomial to describe the background. Only the region below the open charm threshold ($M_{\text{recoil}} < 3.73 \text{ GeV}/c^2$) is included in the fit.

We assess the significance of each signal i using $\sigma_i \equiv \sqrt{-2 \ln(\mathcal{L}_0^i / \mathcal{L}_{\text{max}})}$, where \mathcal{L}_{max} is the maximum likelihood returned by the fit, and \mathcal{L}_0^i is the likelihood with the yield of the state i ($i = \eta_c, \chi_{c0}, \eta_c(2S)$) set to zero. We find $\sigma_{\eta_c} = 6.7$, $\sigma_{\chi_{c0}} = 3.3$ and $\sigma_{\eta_c(2S)} = 3.4$. As the significance of the χ_{c0} and $\eta_c(2S)$ peaks is low, we perform an additional fit using only the η_c shape and the polynomial background: this finds $N_{\eta_c} = 56^{+13}_{-12}$ with $\sigma_{\eta_c} = 5.9$. We use this result, together with the results of fits after varying the charmonium intrinsic widths [13] and the choice of background shape, to estimate the systematic error on the η_c yield due to the fitting procedure.

To determine the $e^+e^- \rightarrow J/\psi \eta_c(\gamma)$ cross-section we correct the signal yield for the reconstruction efficiency obtained from the Monte Carlo. Because of the requirement $N_{\text{ch}} > 4$, the recoil system must contain at least three charged tracks: this removes η_c decays into 0 or 2 charged tracks plus neutrals. As η_c branching fractions are poorly known, we express our result in terms of the product $\sigma(e^+e^- \rightarrow J/\psi \eta_c(\gamma)) \times \mathcal{B}(\eta_c \rightarrow \geq 4 \text{ charged})$, which we find to be $(0.033^{+0.007}_{-0.006} \pm 0.009) \text{ pb}$. Here and elsewhere, the uncertainty quoted second is the systematic error. The various sources of systematic error are listed in Table I, with dominant contributions from the uncertainty in the ISR correction, the choice of fitting procedure, and the production and helicity angle distributions for the J/ψ meson.

To study the $J/\psi c\bar{c}$ mechanism in the region $M_{\text{recoil}} \geq 2m_D$, we search for fully reconstructed D^{*+} and D^0 decays [14] in events with a J/ψ meson. For the study of $J/\psi D^{*+}$ associated production we reconstruct $D^{*+} \rightarrow D^0 \pi^+$ using five D^0 decay modes: $K^-\pi^+$, K^-K^+ , $K^-\pi^-\pi^+\pi^+$, $K_S\pi^+\pi^-$ and $K^-\pi^+\pi^0$. We select D^0 candidates in a $\pm 10 \text{ MeV}/c^2$ mass window for the charged modes and a $\pm 20 \text{ MeV}/c^2$ window for $K^-\pi^+\pi^0$ (approximately 2σ in each case). To improve the $M_{D^0\pi^+}$ resolution D^0 candidates are refitted to the nominal D^0 mass.

Although $B \rightarrow J/\psi X$ decays are rejected by the selection, semileptonic B decays contribute to the background

TABLE I: Sources of systematic error for $\sigma(e^+e^- \rightarrow J/\psi \eta_c)$.

Source	Systematic error (%)
ISR correction	± 19
Fitting procedure	± 16
J/ψ polarization	± 11
Track reconstruction	± 5
Lepton identification	± 4
Total	± 28

under the J/ψ peak and lead to a large D^{*+} signal. To remove the remaining $B\bar{B}$ background we require that either the D^{*+} or one of the leptons from the J/ψ candidate have a momentum above the kinematic limit for B decays: $p_{D^{*+}}^* > 2.6 \text{ GeV}/c$ or $p_{\ell^\pm}^* > 2.6 \text{ GeV}/c$. Choosing the $D^0\pi^+$ combination with the best D^0 mass yields at most one $J/\psi D^{*+}$ candidate per event.

The scatter plot of the dilepton mass versus the $D^0\pi^+$ mass, and the $D^0\pi^+$ mass projection, are shown in Figs. 2a,b. We perform a fit to the $D^0\pi^+$ mass distribution in the J/ψ signal window, with a Gaussian for the D^{*+} signal and a threshold function $A\sqrt{M_{D^0\pi^+} - M_{\text{thres}}}$ for the background. The J/ψ sideband is fit simultaneously, and used to estimate the combinatorial ($\ell^+\ell^-$) D^{*+} contribution to the D^{*+} yield in the signal region. We find $N_{D^{*+}} = 10.5^{+3.6}_{-3.0}$, with a combinatorial contribution of 0.4 ± 0.3 : the signal yield is $10.1^{+3.6}_{-3.0}$, with significance $\sigma_{J/\psi D^{*+} X} = 5.3$. As a cross-check we fit the dilepton mass distribution in the region $2.008 < M_{D^0\pi^+} < 2.012 \text{ GeV}/c^2$, finding $N_{J/\psi} = 9.6^{+3.6}_{-2.9}$. The J/ψ signal shape is fixed from the Monte Carlo simulation and we include a linear background function.

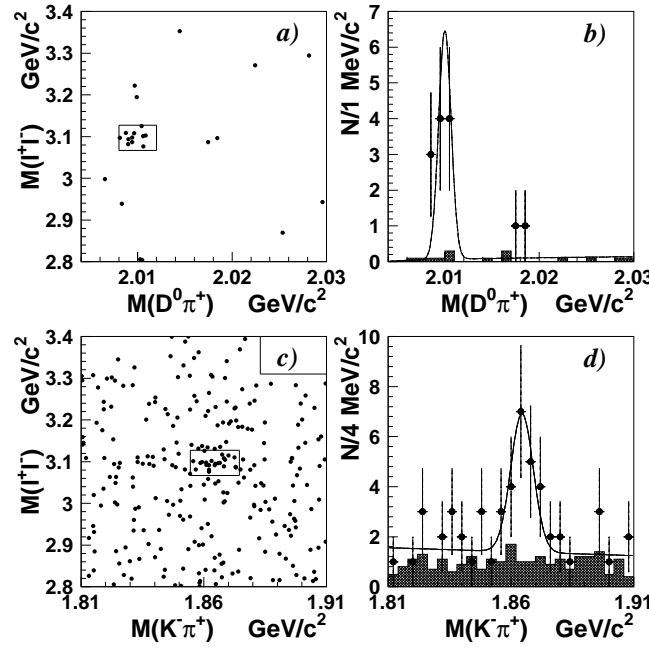


FIG. 2: Results of a search for associated production of J/ψ and charm mesons: a) the scatter plot $M(l^+l^-)$ vs $M(D^0\pi^+)$; b) projection onto the $M(D^0\pi^+)$ axis; c) the scatter plot $M(l^+l^-)$ vs $M(K^-\pi^+(K^+K^-))$; d) projection onto the $M(K^-\pi^+(K^+K^-))$ axis. Points with error bars show the J/ψ signal region and the shaded histograms show the scaled sidebands. The curves represent the fit described in the text.

For the study of $J/\psi D^0$ associated production we use only the cleanest D^0 decay modes $D^0 \rightarrow K^-\pi^+$ and K^-K^+ . As in the $J/\psi D^{*+}$ study, we remove $B\bar{B}$ events by requiring $p_{D^0}^* > 2.6 \text{ GeV}/c$ or $p_{\ell^\pm}^* > 2.6 \text{ GeV}/c$.

A plot of dilepton versus $K^-\pi^+(K^-K^+)$ masses, and the projection onto the $K^-\pi^+(K^-K^+)$ mass axis, are shown in Figs. 2c,d. A simultaneous fit to the $K^-\pi^+(K^-K^+)$ mass distribution in the J/ψ signal window and the sideband finds $N_{D^0} = 15.9^{+5.4}_{-4.7}$ in the signal region, with a combinatorial ($\ell^+\ell^-$) D^0 contribution of 1.0 ± 0.8 . The signal yield is $14.9^{+5.4}_{-4.8}$, with significance $\sigma_{J/\psi D^0 X} = 3.7$. We use a Gaussian signal shape and a linear background function in the fit. As a cross-check, we also fit the dilepton mass spectrum for D^0 signal and sideband regions, obtaining

$N_{J/\psi} = 17.7^{+5.3}_{-4.6}$ and $N_{J/\psi} = 4.3 \pm 0.8$ respectively, where the sideband number is the result of the fit scaled to the expected contribution under the D^0 peak. For all fits the signal shapes are fixed from the Monte Carlo simulation.

To study our reconstruction efficiency for J/ψ mesons produced together with a charmed meson, we generate $e^+e^- \rightarrow J/\psi c\bar{c}$ Monte Carlo events using a simple model adapted from the QQ event generator [15]. Since the efficiency for both particle reconstruction and selection criteria strongly depend on the kinematics, we correct the general kinematic characteristics of the Monte Carlo events to match those of the data using a large sample of continuum J/ψ events. In particular, the distributions of the recoil mass, the J/ψ production and helicity angles, and the angle between the thrust axis of the $c\bar{c}$ system and its boost are adjusted to match the data. These quantities almost fully describe the kinematics of $e^+e^- \rightarrow J/\psi c\bar{c}$. The fragmentation function of $c\bar{c}$ into charmed mesons in each bin of $Q^2(c\bar{c})$ is the only characteristic that has an effect on the efficiency that cannot be determined from the data. We vary the fragmentation function over a wide range, taking the difference in the efficiency into account as a systematic error.

The efficiency is first calculated for $p_{J/\psi}^* > 2.0 \text{ GeV}/c$ and then extrapolated to the full momentum interval, taking into account the cross-sections for inclusive continuum production obtained in Ref. [1] for both $p_{J/\psi}^* > 2.0$ and $p_{J/\psi}^* < 2.0 \text{ GeV}/c$ data. The overall efficiencies for $J/\psi D^{*+}$ and $J/\psi D^0$ are calculated to be $\epsilon_{J/\psi D^{*+}} = (4.1 \pm 1.0) \cdot 10^{-4}$ and $\epsilon_{J/\psi D^0} = (3.7 \pm 0.8) \cdot 10^{-4}$ respectively. Using these values, we find cross-sections $\sigma(e^+e^- \rightarrow J/\psi D^{*+} X) = (0.53^{+0.19}_{-0.15} \pm 0.14) \text{ pb}$ and $\sigma(e^+e^- \rightarrow J/\psi D^0 X) = (0.87^{+0.32}_{-0.28} \pm 0.20) \text{ pb}$. Contributions to the systematic error are summarized in Table II.

According to the Lund model, $c\bar{c}$ fragmentation produces charmed mesons at the rate of 0.53 per event for D^{*+} , and 1.18 per event for D^0 , where both numbers include feed-down from higher states (in particular, $D^{*+} \rightarrow D^0 \pi^+$) [16]. Assuming that these rates apply to $c\bar{c}$ fragmentation in $e^+e^- \rightarrow J/\psi c\bar{c}$, we calculate $\sigma(e^+e^- \rightarrow J/\psi c\bar{c})$ and find $(1.01^{+0.36}_{-0.30} \pm 0.26) \text{ pb}$ and $(0.74^{+0.28}_{-0.24} \pm 0.19) \text{ pb}$ based on our D^{*+} and D^0 measurements, respectively. No systematic error is included for our use of the Lund fragmentation rates. These results are slightly correlated, as two events are common to both samples. Taking this into account, we average the results and obtain $(0.87^{+0.21}_{-0.19} \pm 0.17) \text{ pb}$. In Ref. [1] we found the inclusive prompt J/ψ cross-section to be $\sigma(e^+e^- \rightarrow J/\psi X) = (1.47 \pm 0.10 \pm 0.11) \text{ pb}$, based on a 32.7 fb^{-1} dataset. We therefore infer that a large fraction of prompt J/ψ events, $\sigma(e^+e^- \rightarrow J/\psi c\bar{c})/\sigma(e^+e^- \rightarrow J/\psi X) = 0.59^{+0.15}_{-0.13} \pm 0.12$, is due to the $e^+e^- \rightarrow J/\psi c\bar{c}$ process. Contributions to the systematic error on this ratio are shown in Table II by the numbers in parentheses.

This $J/\psi c\bar{c}$ cross-section is an order of magnitude larger than predicted in Refs. [3, 5, 9], and contradicts the NRQCD expectation that the $J/\psi c\bar{c}$ fraction is small [3, 5]. We note, however, that our result is dependent on the fragmentation model assumed for the $c\bar{c}$ system. In the future, more comprehensive measurements including associated $J/\psi D^+$, $J/\psi D_s^+$ and $J/\psi \Lambda_c^+$ production could significantly reduce this model dependence.

TABLE II: Systematic error contributions for $\sigma(e^+e^- \rightarrow J/\psi D X)$. Numbers in parentheses show contributions to the error on the ratio $\sigma(e^+e^- \rightarrow J/\psi c\bar{c})/\sigma(e^+e^- \rightarrow J/\psi X)$.

Source	Systematic error (%)	
	$J/\psi D^0$	$J/\psi D^{*+}$
MC kinematics correction	± 11 (± 8)	± 10 (± 8)
$c\bar{c}$ fragmentation function	± 8 (± 8)	± 15 (± 15)
Fitting procedure	± 10 (± 10)	± 5 (± 5)
Efficiency of $p_{J/\psi}^*$ cut	± 11 (0)	± 11 (0)
Track reconstruction	± 8 (± 4)	± 12 (± 8)
Lepton and K identification	± 6 (± 3)	± 6 (± 3)
Total	23 (16)	26 (20)

In summary, we have observed both a charmonium state and charmed mesons accompanying prompt J/ψ production in e^+e^- annihilation. We measure $\sigma(e^+e^- \rightarrow J/\psi \eta_c(\gamma)) \times \mathcal{B}(\eta_c \rightarrow \geq 4 \text{ charged}) = (0.033^{+0.007}_{-0.006} \pm 0.009) \text{ pb}$ and $\sigma(e^+e^- \rightarrow J/\psi D^{*+} X) = (0.53^{+0.19}_{-0.15} \pm 0.14) \text{ pb}$, and estimate $\sigma(e^+e^- \rightarrow J/\psi c\bar{c})/\sigma(e^+e^- \rightarrow J/\psi X) = 0.59^{+0.15}_{-0.13} \pm 0.12$. Our results favor $e^+e^- \rightarrow J/\psi c\bar{c}$ as the leading mechanism for prompt J/ψ production at $\sqrt{s} \approx 10.6 \text{ GeV}$.

We wish to thank the KEKB accelerator group for the excellent operation of the KEKB accelerator. We acknowledge support from the Ministry of Education, Culture, Sports, Science, and Technology of Japan and the Japan Society for the Promotion of Science; the Australian Research Council and the Australian Department of Industry, Science and Resources; the National Science Foundation of China under contract No. 10175071; the Department of Science and Technology of India; the BK21 program of the Ministry of Education of Korea and the CHEP SRC program of

the Korea Science and Engineering Foundation; the Polish State Committee for Scientific Research under contract No. 2P03B 17017; the Ministry of Science and Technology of the Russian Federation; the Ministry of Education, Science and Sport of the Republic of Slovenia; the National Science Council and the Ministry of Education of Taiwan; and the U.S. Department of Energy.

* on leave from Nova Gorica Polytechnic, Slovenia

† on leave from University of Toronto, Toronto ON

- [1] K. Abe *et al.* (Belle Collab.), Phys. Rev. Lett. **88**, 052001 (2002).
- [2] E. Braaten and S. Fleming, Phys. Rev. Lett. **74**, 3327 (1995); P. Cho and M. Wise, Phys. Lett. **B346**, 129 (1995); M. Cacciari, M. Greco, M. L. Mangano, and A. Petrelli, *ibid.* **B356**, 553 (1995).
- [3] P. Cho and A. K. Leibovich, Phys. Rev. D **53**, 150 (1996); **53**, 6203 (1996). S. Baek, P. Ko, J. Lee, and H. S. Song, J. Kor. Phys. Soc. **33**, 97 (1998); hep-ph/9804455.
- [4] E. Braaten and Yu-Qi Chen, Phys. Rev. Lett. **76**, 730 (1996).
- [5] F. Yuan, C.-F. Qiao, and K.-T. Chao, Phys. Rev. D **56**, 321 (1997).
- [6] B. Aubert *et al.* (BaBar Collab.), Phys. Rev. Lett. **87** 162002 (2001).
- [7] Y. Iwasaki, Phys. Rev. D **16**, 220 (1977) .
- [8] G. L. Kane, J. P. Leveille, and D. M. Scott, Phys. Lett. **B85**, 115 (1979).
- [9] V. V. Kiselev, A. K. Likhoded, and M. V. Shevlyagin, Phys. Lett. **B332**, 411 (1994).
- [10] KEKB B Factory Design Report, KEK Report 95-7, 1995 (unpublished); Y. Funakoshi *et al.*, Proc. 2000 European Particle Accelerator Conference, Vienna 2000.
- [11] A. Abashian *et al.* (Belle Collab.), Nucl. Instr. and Meth. **A479**, 117 (2002).
- [12] W. Buchmüller and S.-H. H. Tye, Phys. Rev. D. **24**, 132 (1981); S. Godfrey and N. Isgur, *ibid.* **32**, 189 (1985).
- [13] D.E. Groom *et al.*, Eur. Phys. J. **C15**, 1 (2000).
- [14] Charge-conjugated modes are implicitly included.
- [15] QQ was developed by the CLEO Collaboration. See <http://www.lns.cornell.edu/public/CLEO/soft/qq>.
- [16] T. Sjöstrand, PYTHIA 5.7 / JETSET 7.4, Comp. Phys. Commun. **82**, 74 (1994). The D^{*+}/D^0 ratio is constant over \sqrt{s} except for a decrease near D^{*+} mass threshold: the effect on the result is negligible.